9356 *Inorg. Chem.* **2009**, *48*, 9356–9364
DOI: 10.1021/ic901160v

Inorganic Chemistry
Article

Synthesis, Structural Characterization, and Biological Evaluation of Oxorhenium(V) Complexes with a Novel Type of Thiosemicarbazones Derived from *N*-[*N*′,*N*′-Dialkylamino(thiocarbonyl)]benzimidoyl Chlorides

Hung Huy Nguyen,[†,⊥] Jesudas J. Jegathesh,[‡] Pedro I. da S. Maia,[§] Victor M. Deflon,[§] Ronald Gust,[∥] Silke Bergemann,[∥] and Ulrich Abram*[,‡]

[†]*Department of Chemistry, Hanoi University of Sciences, 19 Le Thanh Tong, Hanoi, Vietnam,* [‡]*Freie Universität Berlin, Institute of Chemistry and Biochemistry, Fabeckstrasse 34-36, D-14195 Berlin, Germany,* [§]*Instituto de Química de São Carlos, Universidade de São Paulo, CP 780 São Carlos − São Paulo, Brazil, and* [∥]*Institute of Pharmacy, Königin-Luise-Strasse 2 and 4, 14195 Berlin, Germany.* [⊥]*Present address: Freie Universität Berlin, Institute of Chemistry and Biochemistry.*

Received June 17, 2009

Reactions of *N*-[*N*′,*N*′-diethylamino(thiocarbonyl)]benzimidoyl chloride with 4,4-dialkylthiosemicarbazides give a novel class of thiosemicarbazides/thiosemicarbazones, H_2L, which causes a remarkable reduction of cell growth in *in vitro* experiments. These strong antiproliferative effects are also observed for oxorhenium(V) complexes of the general composition [ReOCl(L)], which are formed by reactions of the potentially tridentate ligands with $(NBu_4)[ReOCl_4]$. A systematic substitution of the alkyl groups in the thiosemicarbazone building blocks of the ligands do not significantly influence the biological activity of the metal complexes, while the replacement of the chloro ligand by a PPh_3 ligand (by the replacement of the oxo unit by a nitrido ligand) completely terminated the cytotoxicity of the metal complexes.

Introduction

Thiosemicarbazones, which form stable complexes with many main group and transition metals,[1] constantly attract the interest of chemists and pharmacists because of their remarkable biological and pharmacological properties such as antibacterial, antiviral, antineoplastic, or antimalarial activity.[2] Modifications of the thiosemicarbazone framework, to find new compounds with higher activity and/or to tune their biological activity, have been extensively studied, and relationships between the biological activity and chelate formation are evident in a number of cases.[3] This makes structural studies more interesting, which are the rational base for structure−activity relationships (SAR).

Chart 1. Thiosemicarbazones of Biological Interest

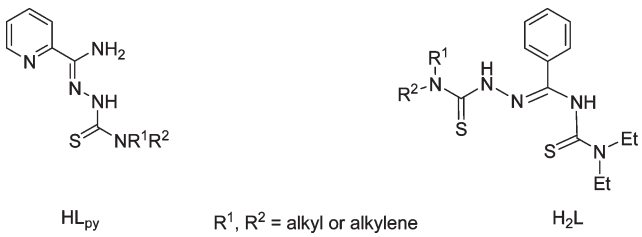

HL_{py} R^1, R^2 = alkyl or alkylene H_2L

Surprisingly little is known about thiosemicarbazone complexes with rhenium and technetium. Particularly in the chemistry of the high oxidation states of these metals, the reducing capacity of thiosemicarbazones frequently makes reactions uncontrollable, and ligand decomposition is observed. Hitherto, only one stable rhenium(V) oxo complex with 2-pyridine formamide thiosemicarbazone (HL_{py}, see Chart 1) is structurally characterized.[4] Very recently, we reported two representatives of a new class of thiosemicarbazones (H_2L, see Chart 1) and their technetium(V) oxo complexes.[5] The novel ligands possess in addition to the thiosemicarbazone moiety a thiourea building block derived from *N*-[*N*′,*N*′-diethylamino(thiocarbonyl)]benzimidoyl chloride. This allows delocalization of electron density to a large extent, and consequently they can conform the

*To whom correspondence should be addressed. E-mail: abram@chemie.fu-berlin.de. Phone: (#49) 30 83854002. Fax: (#49) 30 83852676.

(1) (a) Campbell, M. J. M. *Coord. Chem. Rev.* **1975**, *15*, 279. (b) West, D. X.; Padhye, S. B.; Sonawane, P. A. *Struct. Bonding (Berlin)* **1991**, *76*, 1. (c) Casas, J. S.; García-Tasende, M. S.; Sordo, J. *Coord. Chem. Rev.* **2000**, *209*, 49.

(2) (a) Klayman, D. L.; Scovill, J. B.; Bartosevich, J. F.; Bruce, J. *J. Med. Chem.* **1983**, *26*, 39. (b) Dobek, A. S.; Klayman, D. L.; Dickson, E. T.; Scovill, J. P.; Oster, C. N. *Arzneim.-Forsch.* **1983**, *33*, 1583. (c) Klayman, D. L.; Scovill, J. P.; Mason, C. J.; Bartosevich, J. F.; Bruce, J.; Lin, A. *Arzneim.-Forsch.* **1983**, *33*, 909. (d) Klayman, D. L.; Scovill, J. P.; Bartosevich, J. F.; Mason, C. J. *J. Med. Chem.* **1979**, *22*, 1367. (e) Shipman, C., Jr.; Smith, S. H.; Drach, J. C.; Klayman, D. L. *Antiviral Res.* **1986**, *6*, 197.

(3) (a) Miertus, S.; Filipovic, P. *Eur. J. Med. Chem.* **1982**, *17*, 145. (b) Saryan, L. A.; Mailer, K.; Krishnamurti, C.; Atholine, W.; Petering, D. H. *Biochem. Pharmacol.* **1981**, *30*, 1595. (c) Sartorelli, A. C.; Agrawal, K. A.; Tsiftsoglou, A. S.; Moore, E. C. *Adv. Enzyme Regul.* **1977**, *15*, 117. (d) Scovill, L. P.; Klayman, D. L.; Lambrose, C.; Childs, G. E.; Notsch, J. D. *J. Med. Chem.* **1984**, *27*, 87.

(4) Garcia Santos, I.; Abram, U. *Z. Anorg. Allg. Chem.* **2004**, *630*, 697.

(5) Nguyen, H. H.; da S. Maia, P. I.; Deflon, V. M.; Abram, U. *Inorg. Chem.* **2009**, *48*, 25.

 Published on Web 09/08/2009

Scheme 1. Synthesis of H_2L

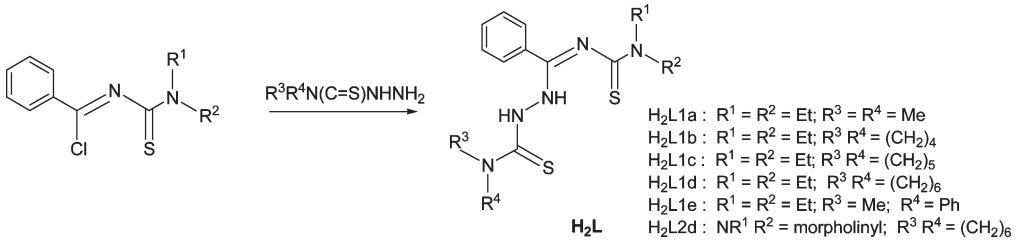

electronic requirements of the metal ions in a large scale. The fact that oxotechnetium(V) complexes are stable, encouraged us to synthesize a reasonable number of such compounds and their rhenium analogues. With regard to the higher oxidation potential of the TcO^{3+} core compared to the ReO^{3+} unit,[6] reduction of the rhenium core should not be expected.

In the present paper, we devote our interest to the coordination chemistry of the novel ligand system with rhenium and the biological behavior of the thiosemicarbazone derivatives and their rhenium complexes. The ligands H_2L can easily be modified by different substituents R^1 and R^2 of the thiosemicarbazide moiety. Additionally, variation of the dialkylamino group of the thiourea building block is possible and allows a smooth tuning of the molecular properties. Modification of the metal core ReO^{3+} versus ReN^{2+} gives another opportunity to study SARs. Thus, we have prepared a series of H_2L and corresponding rhenium complexes and studied their basic coordination chemistry, as well as the cytotoxicity of the obtained compounds. The radiopharmaceutical potential of the rhenium complexes and their technetium analogues, which are described in ref 5, shall not be subject of this communication but will be tested in future work.

Results and Discussion

N-[*N*′,*N*′-Dialkylamino(thiocarbonyl)]benzimidoyl chlorides are known as reactive synthons, which easily react with ammonia or primary amines to form benzamidine-type compounds. To develop new types of benzamidines, which are potentially useful as pharmaceuticals, we combined the thiourea building blocks of the benzimidoyl chlorides with a bioactive class of substances: 4,4-dialkylthiosemicarbazides. The expected product will contain both thiourea and thiosemicarbazone moieties. It was hoped that the presence of an additional thiourea group in the products would influence the bioactivities and/or at least will improve the coordination properties of the new compounds to metal ions by the introduction of an additional donor site.

Thus, the reactions of appropriate *N*-[*N*′,*N*′-dialkylamino-(thiocarbonyl)] benzimidoyl chlorides and a series of 4,4-dialkylthiosemicarbazides were studied. The reactions proceed quickly in dry acetone at ambient temperature and give tridentate benzamidine ligands of the type H_2L in high yields (Scheme 1). The progress of the reaction can readily be checked by thin-layer chromatography on alumina and is conveniently indicated by the formation of a colorless precipitate, $NEt_3 \cdot HCl$, which is almost insoluble in acetone. All products were isolated as colorless, analytically pure, crystalline solids directly from the reaction mixtures.

The IR spectra of the H_2L compounds reveal broad, strong absorptions in the range between 3170 and 3210 cm^{-1} of the NH stretches and very strong absorptions in the region between 1610 and 1640 cm^{-1}, which can be assigned to the C=N vibrations.[7] C=S stretching vibrations cannot be assigned unambiguously in the compounds under study.

The ^1H NMR spectra of the free ligands show two sets of well separated signals corresponding to their ethyl residues, which is due to the hindered rotation around of the $C-NEt_2$ bonds of the thiourea moieties as has been discussed before.[5] The rotation around the $C-NR^1R^2$ bonds of the thiosemicarbazide units in most of the ligands is not restricted as is indicated by the appearance of magnetically equivalent protons. The signals of the two NH protons appear as very broad singlets in the region between 9.5 and 10.1 ppm. In the ^{13}C NMR spectra, the C=N and C=S signals of thiourea residues appear in the regions around 149 ppm and 183 ppm, while the C=S resonances of thiosemicarbazide moiety appear around 179 ppm.

Representatives of H_2L were studied by X-ray analysis. Figure 1 depicts the molecular structure of H_2L1b. Selected bond lengths and angles are summarized in Table 1. The protonation of the nitrogen atoms N3 and N7 is experimentally justified by the detection of peaks of electron density in the final Fourier map, which can be assigned to corresponding hydrogen atoms, and the fact that they are involved into hydrogen bonds. The bonding arrangement of the H_2L1b skeleton is consistent with C4−N5 bond lengths of 1.286/1.285 Å, which can be assigned to a C=N double bond and C4−N3 distances of 1.416/1.431 Å, which is typical for C−N single bonds. This bonding arrangement in the solid state of H_2L1b results in a "thiosemicarbazone" (tautomeric form ***C*** of Chart 2) rather than a "thiosemicarbazide". This is in contrast to the situation in the solid-state molecular structure of H_2L1a,[5] which has been determined recently and contains a double bond between C4 and N3 and a single bond between C4 and N5. Consequently the protons were found at the atoms N5 and N7, and the compound is best described with the tautomeric form ***A*** in Chart 2.

It is interesting to note that both structures reveal the same molecular arrangement, meaning a configuration, which allows an intramolecular hydrogen bond between the atoms N7 and S1. The remaining acidic proton can then be located on either N3 or N5, which most probably is controlled by the possibility of the formation of intermolecular hydrogen bonds. Thus, H_2L should finally be treated as between "thiosemicarbazide" and "thiosemicarbazone", and the solid

(6) (a) Alberto, R. Technetium. In *Comprehensive Coordination Chemistry II*; McCleverty, J. A., Meyer, T. J., Eds.; Elsevier: Amsterdam, The Netherlands, 2004; p 127. (b) Abram, U. Rhenium. In *Comprehensive Coordination Chemistry II*; McCleverty, J. A., Meyer, T. J., Eds.; Elsevier: Amsterdam, The Netherlands, 2003; Vol. *5*, p 271.

(7) Nguyen, H. H.; Grewe, J.; Schroer, J.; Kuhn, B.; Abram, U. *Inorg. Chem.* **2008**, *47*, 5136.

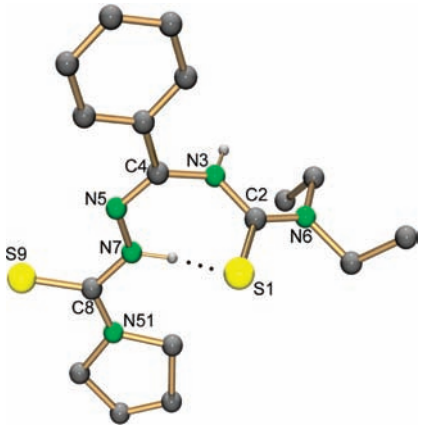

Figure 1. Molecular structure of H_2L1b.[8] Hydrogen atoms except of those bonded to nitrogen are omitted for clarity.

Table 1. Selected Bond Lengths (Å) and Angles (deg) in H_2L1b[a]

S1−C2	1.692(4)/1.685(3)	N5−N7	1.374(4)/1.365(3)
C2−N3	1.372(4)/1.372(4)	N7−C8	1.361(4)/1.357(4)
N3−C4	1.417(4)/1.429(4)	C8−S9	1.680(3)/1.683(3)
C4−N5	1.285(4)/1.281(4)	C8−N51	1.342(4)/1.339(4)
C2−N6	1.337(4)/1.346(4)		

H bonds	*d*(D-H)	*d*(H···A)	*d*(D···A)
N7−H7···S1	0.86/0.86	2.88/3.05	3.238(3)/3.389(3)
N3−H3−S9[b]	0.86/0.86	2.59/2.70	3.378(3)/3.433(3)

[a] Values for two crystallographically independent molecules. [b] Symmetry transformations used to generate equivalent atoms: #1 $x, y-1, z$; #2 $x, y+1, z$.

Chart 2. Possible Conformations of H_2L

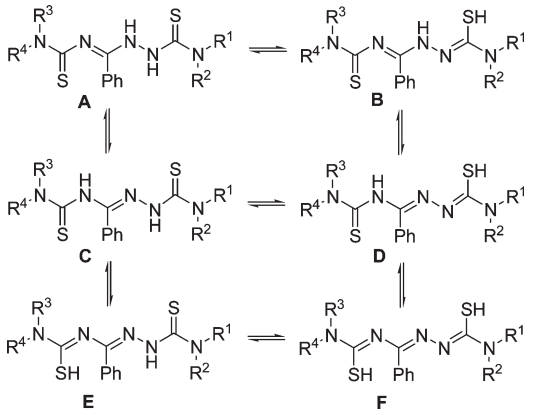

state structures of the compounds do not represent a suitable tool to predict the situation in metal complexes of the compounds. In solution and in the metal complexes of the new ligands, other mesomeric forms should also be considered as shown in Chart 2. Particularly when chelate formation establishes an extended system of delocalized π-electron density, the bonding situation might be different from that in Figure 1.

Treatment of $(NBu_4)[ReOCl_4]$ with an equivalent amount of H_2L in methanol at room temperature affords red solids of the composition [ReOCl(L1)] (**1**) and [ReOCl(L2)] (**2**) in excellent yields (Scheme 2). The compounds are stable both in solution and in the solid state. Infrared spectra of

(8) Farrugia, L. J. *J. Appl. Crystallogr.* **1997**, *30*, 565.

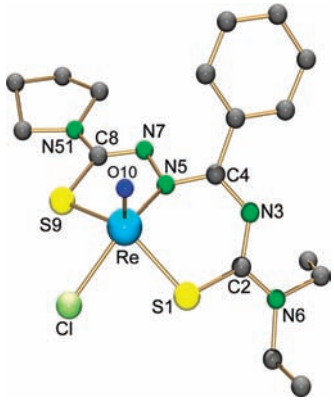

Figure 2. Structure of the complex **1b**.[8] Hydrogen atoms are omitted for clarity.

Scheme 2. Synthesis of the Oxorhenium(V) Complexes

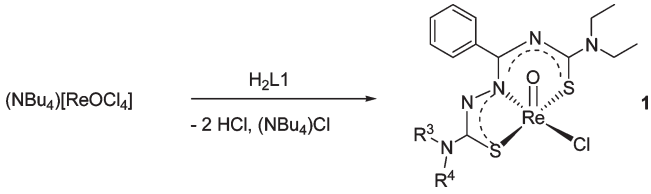

complexes **1** exhibit strong bathochromic shifts of the $\nu_{C=N}$ stretches of H_2L into the region near 1520 cm^{-1}, which indicates chelate formation with a large degree of π-electron delocalization within the chelate rings.

The absence of ν_{NH} bands indicates the expected double deprotonation of the ligands during complex formation. Intense bands appearing at the range between 979 and 983 cm^{-1} can be assigned to the Re=O vibrations. ^1H NMR spectra of the complexes, similar to the spectra of the uncoordinated thiosemicarbazones, show two well-separated sets of signals of the ethyl groups or morpholine moiety of the thiourea unit and no hindered rotation effects for the C-NR^1R^2 moieties of the thiosemicarbazide side. Mass spectra of complexes do not show the molecular ion peak. The exchange of chloro ligands by the solvent MeOH is observed in all spectra and intense peaks corresponding to $[M - HCl + MeOH + Na]^+$ cations appear.

Figure 2 represents the molecular structure of **1b** as a representative compound of the [ReOCl(L)] complexes. More complexes have been studied crystallographically, and selected bond lengths and angles for some analogous compounds are compared in Table 2. The atomic labeling scheme for all compounds has been adopted from the complex **1b** shown in Figure 2. The coordination environment of the rhenium atoms is best described as distorted square pyramids with the oxo ligands in apical positions. The basal planes are defined by the donor atoms of the tridentate ligands and a remaining chloro ligand. The rhenium atoms are situated between 0.715(2) and 0.735(2) Å above this plane toward the oxo ligands. All O10−Re−X angles (X = equatorial donor atom) fall in the range between 103 and 112°. The maximum Re−O10 distance in the compounds under study is 1.694(7) Å for **1e**, which is still within the expected range for a rhenium−oxygen double bond.[6b] A considerable delocalization of π-electron density in the six-membered ring is observed. The C−S and C−N bond distances inside the chelate rings are all within the ranges between carbon−sulfur

Table 2. Selected Bond Lengths (Å) and Angles (deg) in [ReOCl(L1)] Complexes (**1**)[a]

	1b	1d	1e		1b	1d	1e
Re−O10	1.652(7)	1.657(8)	1.694(7)	N3−C4	1.312(1)	1.31(1)	1.31(1)
Re−S1	2.307(2)	2.298(2)	2.300(2)	C4−N5	1.36(1)	1.35(1)	1.37(1)
Re−N5	2.000(6)	2.035(7)	2.005(7)	C2−N6	1.30(1)	1.29(1)	1.32(1)
Re−S9	2.283(2)	2.282(2)	2.287(2)	N5−N7	1.430(9)	1.41(1)	1.41(1)
Re−Cl	2.364(2)	2.357(3)	2.361(2)	N7−C8	1.272(11)	1.29(1)	1.29(1)
S1−C2	1.76(1)	1.748(9)	1.764(9)	C8−S9	1.778(9)	1.770(9)	1.77(1)
C2−N3	1.35(1)	1.36(1)	1.35(1)	C8−N51	1.35(1)	1.35(1)	1.38(1)
O10−Re−S1	111.8(3)	109.6(3)	111.7(3)	N5−Re−S9	80.6(2)	79.9(2)	80.6(2)
O10−Re−N5	106.4(3)	106.4(3)	103.9(3)	S9−Re−Cl	84.3(1)	83.7(1)	85.0(1)
O10−Re−S9	112.8(3)	109.7(3)	112.4(3)	Cl−Re−S1	81.2(1)	80.7(1)	81.8(1)
O10−Re−Cl	105.7(3)	108.9(3)	105.0(3)	S1−Re−S9	135.3(1)	140.6(1)	135.8(1)
S1−Re−N5	89.8(2)	92.2(2)	91.1(2)	N5−Re−Cl	147.7(2)	144.4(2)	150.9(2)

[a] For the atomic labeling scheme see Figure 2.

and carbon−nitrogen single and double bonds. This bond length equalization is even extended to the C2−N6 bonds, which are significantly shorter than expected for typical single bonds. The partial transfer of electron density into this bond agrees with the ^{1}H NMR spectra. In the five-membered rings, the C8−N7 bonds, which fall into the range between 1.27(1) and 1.29(1) Å have more double bond character than those in the uncoordinated thiosemicarbazones/thiosemicarbazides. While the C−S distances in H_2L1b are almost equal, the C8−S9 bonds are a little longer than the C2−S1 distances in the complexes. This accompanies the fact that the Re−S9 bond lengths are slightly shorter than Re−S1 distances. Nevertheless, the bonding arrangement of the ligands in the complexes is best described as borderline between the "thiosemicarbazide-type" and the "thiosemicarbazone-type".

All complexes of the type **1** are only distinguished by the substituents R^3 and R^4 of the thiosemicarbazide side, while an additional modification was introduced at the residues R^1 and R^2 in the H_2L2d and the corresponding oxorhenium(V) complex **2d**. The replacement of the oxo ligand "O^{2-}" by a nitrido ligand "N^{3-}", however, gives access to a completely new class of rhenium(V) complexes with the novel ligands, and thus the opportunity to study the biological properties of the ligands in another coordination environment.

[$ReNCl_2(PPh_3)_2$] is a common Re(V) nitrido starting material. The compound is sparingly soluble in organic solvents. However, it slowly dissolves and forms deep red solutions, when suspensions with H_2L1d or H_2L2d in CH_2Cl_2 are stirred at room temperature (Scheme 3). The addition of a supporting base like Et_3N accelerates the consumption of [$ReNCl_2(PPh_3)_2$] and yields the same products: [Re(N)(L1)-(PPh_3)] (**3**) or [Re(N)(L2)(PPh_3)] (**4d**). The products were studied by common spectroscopic methods. The IR spectra of the products reveal strong bathochromic shifts of the $\nu_{C=N}$ bands and the absence of ν_{NH} absorptions indicate the expected formation of dianionic ligands. ^{1}H NMR spectra of **3** and **4d** have the same patterns as discussed for the corresponding complexes **1** and **2**, except that additionally poorly resolved resonances of triphenylphosphine ligands are present. The presence of coordinated PPh_3 is also confirmed by singlets in the region around 33 ppm in the ^{31}P{H} NMR spectra. The mass spectra of **3d** and **4d** exhibit intense molecular ion peaks with the expected isotopic patterns for $^{185/187}$Re.

Scheme 3. Synthesis of the Nitridorhenium(V) Complexes

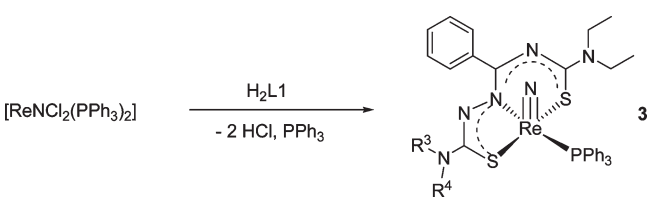

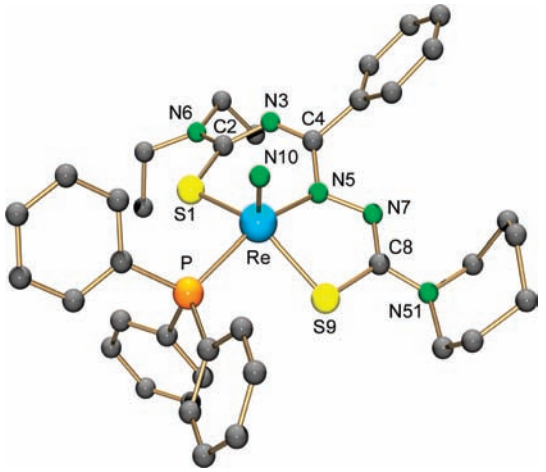

Figure 3. Structure of the complex **3d**.[8] Hydrogen atoms are omitted for clarity.

Table 3. Selected Bond Lengths (Å) and Angles (deg) in **3d**

Re−N10	1.658(5)	N3−C4	1.324(8)
Re−S1	2.339(1)	C4−N5	1.326(7)
Re−N5	2.082(4)	C2−N6	1.347(8)
Re−S9	2.330(1)	N5−N7	1.437(7)
Re−P	2.397(1)	N7−C8	1.291(7)
S1−C2	1.752(6)	C8−S9	1.779(6)
C2−N3	1.316(8)	C8−N51	1.367(7)
N10−Re−S1	108.6(2)	N5−Re−S9	79.9(1)
N10−Re−N5	106.9(2)	S9−Re−P	88.3(1)
N10−Re−S9	109.5(2)	P−Re−S1	86.4(1)
N10−Re−P	97.4(2)	S1−Re−S9	141.9(1)
S1−Re−N5	89.6(1)	N5−Re−P	155.4(1)

Single crystals of **3d**, which were suitable for X-ray structure analysis were obtained by slow evaporation of a CH_2Cl_2/MeOH solution of the compound. Figure 3 illustrates the molecular structure of **3d**. Selected bond lengths and angles for the complex are presented in Table 3. The rhenium atom is coordinated in a distorted square-pyramidal environment with a nitrido ligand in apical position. The tridentate ligand $(L1d)^{2-}$ is arranged in the equatorial plane and binds to the

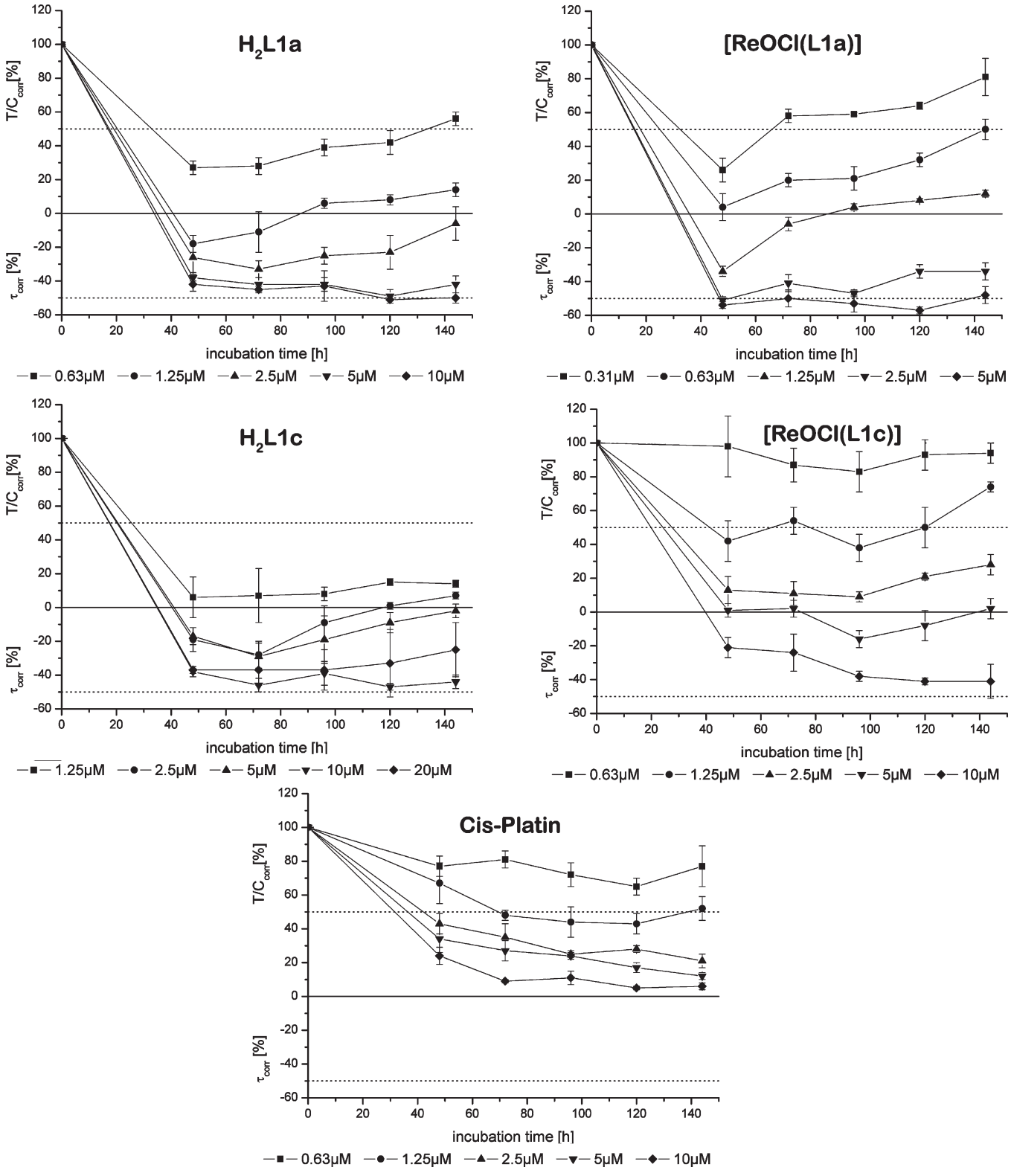

Figure 4. Cytotoxic effects of selected ligands and complexes.

rhenium atom via the atoms S1, N5, and S9, as has been observed in the oxo complexes **1**. The remaining equatorial coordination position is occupied by a PPh_3 ligand. The Re atom lies about 0.615(1) Å above this plane toward the nitrido ligand. The Re−N10 bond distance of 1.658(5) Å is in the expected range of Re≡N triple bonds. The bonding situation of the chelate ring of $(L1d)^{2-}$ in **3d** is similar to that discussed for the complexes of type **1**. All Re−S and Re−N bonds in **3d** are slightly longer than those in the corresponding oxo complex **1d**, indicating that the transfer of electron density from the organic ligand to the metal ion is slightly less in the nitrido species than in the oxo compounds. This is not unexpected in the light that the nitrido ligand is a stronger π donor than the oxo ligand.[8]

With the novel thiosemicarbazones H_2L and their oxo complexes [ReOCl(L)] and the corresponding nitrido complexes [ReN(L)(PPh_3)], there exists a series of familiar compounds, which are worth to be studied for their biological activity. To obtain an overview of the influence of the individual residues in the molecular framework of the thiosemicarbazones, we first modified R^1 and R^2 (compounds **1d** and **2d**). Since first tests showed a similar behavior for such representatives, we decided to prepare a larger number of compounds modifying the residues R^3 and R^4 (compounds H_2L1a to H_2L1e) and their corresponding rhenium complexes. The use of different coordination environments in the metal complexes (oxo compound vs nitrido complexes) may allow an insight into the mechanism of potential activity.

Thiosemicarbazones exhibit various biological activities and have therefore attracted considerable pharmaceutical interest. Several mechanisms of antitumor action were proposed and compelled the interest of an SAR study. Furthermore, it is well-known that such compounds are potent metal chelators, and the cytotoxic properties of the compounds are influenced by chelation. In many cases, an increased activity of the metal complexes is observed, which is assumed to be an effect of a metal-assisted transport, while complex dissociation inside the cell releases the thiosemicarbazones as the biologically active species.[3d] Thus, we investigated the antiproliferative effects of the ligands H_2L1 and H_2L2 in relation to their rhenium complexes in a time response as well as in a concentration response assay. From the first study the response of the cells to the compounds can be estimated, while the latter allows the calculation of IC_{50} values.

The thiosemicarbazone H_2L1a causes a strong reduction of the growth of human MCF-7 breast cancer cells. Maximum activity was already detected after an incubation time of 48 h (Figure 4). At the concentrations of 1.25 to 10 μM cytocidal effects were observed. The rising recuperation of the cells at lower concentrations is characteristic for a cytostatic effect. The time response curve of cisplatin is quite different, with a maximum cytotoxicity appearing not before an incubation time of more than 100 h. All compounds H_2L1 and H_2L2 show this interesting behavior and comparable time response curves, which allowed the comparison of IC_{50} values (after an incubation time of 48 h, see Table 4).

The degree of cytotoxicity can be influenced by the variation of the peripheral substituents R^1 and R^2 as well as R^3 and R^4. The IC_{50} value of H_2L1a was 0.39 μM. The replacement of an N-methyl group with a R^4 = phenyl (H_2L1e: IC_{50} = 0.85 μM) or the replacement of the *N*,*N*-dimethyl group with a pyrrolidine (H_2L1b: IC_{50} = 2.21 μM) reduced the cytotoxicity. Interestingly, the ring size (5-membered ring to 7-membered ring) determined the antiproliferative effects. The IC_{50} value of the piperidine derivative H_2L1c (0.17 μM) is lower than that of H_2L1b and H_2L1a, while that of the azepine derivative H_2L1d was comparable to H_2L1b. Finally, the exchange of the *N*,*N*-diethyl moiety of H_2L1d by morpholine increased the cytotoxicity (H_2L2d: IC_{50} = 0.73 μM).

After coordination of the ligands to an oxorhenium(V) center, no clear trend in biological activity was observed. All [ReOCl(L)] complexes show significant toxic effects. In the case of [ReOCl(L1a)], and [ReOCl(L1d)], there was no (or almost no) change of cytotoxicity with respect to their noncoordinated thiosemicarbazones. The effects of [ReOCl(L1c)] and [ReOCl(L2d)], however, were lower than that of the corresponding thiosemicarbazones. This suggests different mechanisms for the biological activities of the uncoordinated thiosemicarbazones and their related rhenium complexes, and is also supported by the differences between the oxo and nitrido complexes. A detailed discussion, however, would contain too much speculation and shall not be done on the basis of the present data.

Table 4. Cytotoxic Effects of Ligands H_2L and Complexes [ReOCl(L)] against MCF-7 Cells

					IC_{50} [μM]	
	R^1	R^2	R^3	R^4	ligand	[ReOCl(L)] complex
H_2L1a	Et	Et	CH_3	CH_3	0.39(5)	0.39(3)
H_2L1b	Et	Et	$(CH_2)_4$		2.21(36)	2.52(18)
H_2L1c	Et	Et	$(CH_2)_5$		0.17(5)	1.13(18)
H_2L1d	Et	Et	$(CH_2)_6$		2.43(28)	1.51(17)
H_2L1e	Et	Et	CH_3	C_6H_5	0.85(7)	0.41(2)
H_2L2d	morpholinyl		$(CH_2)_6$		0.75(8)	4.43(6)

A clear experimental result, however, is the fact, that the replacement of the "O^{2-}" by a nitrido "N^{3-}" ligand and the chloro ligand by a triphenylphosphine completely terminates the cytotoxicity of the complexes. The complexes **3** are even inactive at the highest concentration used (20 μM). Since also a steric repulsion from possible targets because of the voluminous triphenylphosphine ligand can not be excluded, a detailed study on the non-activity of the nitrido compounds and the mode of action of the oxo complexes is necessary and will be subject of future work.

Presently, studies with further systematic variations of the molecular framework are underway in our laboratories. They also include the quest for the point of attack of the active compounds and the role of the metal ion and the intracellular targets. For example thiosemicarbazones can stabilize cleavable complexes formed by topoisomerase II (topoII) and DNA leading to apoptosis or they can inhibit ribonucleotide reductase (RR) activity.[9] Studies with structurally analogue technetium complexes and/or the beta-emitting rhenium isotopes ^{186}Re or ^{188}Re will help to answer the remaining questions and allow further optimization of the promising cancerostatic properties of the new class of complexes.

Experimental Section

Materials. All reagents used in this study were reagent grade and used without further purification. Solvents were dried and freshly distilled prior to use unless otherwise stated. (NBu_4)[$ReOCl_4$] and [$ReNCl_2(PPh_3)_2$] was prepared by published methods.[10,11] 4,4-Dialkylthiosemicarbazides and *N*-[*N*′,*N*′-dialkylamino(thiocarbonyl)]benzimidoyl chlorides were synthesized by standard procedures.[12,13]

Physical Measurements. Infrared spectra were measured as KBr pellets on a Shimadzu FTIR-spectrometer between 400 and 4000 cm^{-1}. ESI mass spectra were measured with an Agilent 6210 ESI-TOF. All MS results are given in the form: *m*/*z*, assignment. Elemental analysis of carbon, hydrogen, nitrogen, and sulfur were determined using a Heraeus vario EL elemental

(9) Chen, J.; Huang, Y.-W.; Liu, G.; Afrasiabi, Z.; Sinn, E.; Padhye, S.; Ma, Y. *Toxicol. Appl. Pharmacol.* **2004**, *197*, 40.
(10) Alberto, R.; Schibli, R.; Egli, A.; Schubiger, P. A.; Herrmann, W. A.; Artus, G.; Abram, U.; Kaden, T. A. *J. Organomet. Chem.* **1995**, *217*, 492.
(11) Chatt, J.; Falk, C. D.; Leight, G. J.; Paske, R. J. *J. Chem. Soc. A* **1969**, 2288.
(12) Sreekanth, A.; Fun, H.-K. *J. Mol. Struct.* **2005**, *737*, 61.
(13) (a) Beyer, L; Widera, R. *Tetrahedron Lett.* **1982**, *23*, 1881. (b) Beyer, L.; Hartung, J.; Widera, R. *Tetrahedron* **1984**, *40*, 405.

analyzer. Some values of the elemental analyses of the rhenium complexes significantly differ from the calculated values. This seems to be a systematic problem probably caused by some hydride and/or carbide formation during the combustion process and does not refer to impure samples. Reference samples have been checked by high resolution mass spectrometry. NMR-spectra were taken with a JEOL 400 MHz multinuclear spectrometer.

Syntheses of the Ligands. *N*-[*N*′,*N*′-Dialkylamino(thiocarbonyl)]benzimidoyl chloride (5 mmol) was dissolved in 10 mL of dry acetone and slowly added to a stirred mixture of 4,4-dialkylthiosemicarbazide (5 mmol) and NEt_3 (1.51 g, 15 mmol) in 10 mL of dry acetone. The mixture was stirred for 4 h at room temperature. The formed precipitate of $NEt_3 \cdot HCl$ was filtered off, and the filtrate was evaporated to dryness under reduced pressure. The residue was redissolved in 5 mL of CH_2Cl_2, and the obtained solution was extracted with brine solution (3 × 5 mL). After being dried with $MgSO_4$, the organic solvent was removed under vacuum. Diethylether (10 mL) was added, and the mixture was stored at −20 °C for 1 day. The colorless solid of H_2L, which deposited from this solution, was filtered off, washed with diethylether, and then recrystallized from a mixture of CH_2Cl_2/*n*-hexane.

Data for H_2L1a ($R^1 = R^2 = Et$, $R^3 = R^4 = Me$). Yield: 75% (1.237 g). Anal. Calcd for $C_{15}H_{23}N_5S_2$: C, 53.38; H, 6.87; N, 20.75; S, 19.00%. Found: C, 53.80; H, 6.69; N, 21.02; S, 19.02%. IR (ν in cm^{-1}): 3182 m (N−H), 1635 s (C=N). ^{1}H NMR ($CDCl_3$, δ, ppm): 1.24 (t, J = 7.2 Hz, 3 H, CH_3), 1.36 (t, J = 7.2 Hz, 3 H, CH_3), 3.28 (s, 6 H, N−CH_3), 3.54 (q, J = 7.2 Hz, 2 H, CH_2), 3.90 (q, J = 7.1 Hz, 2 H, CH_2), 7.41−7.48 (m, 3 H, Ph), 7.90 (d, J = 8.3 Hz, 2 H, o-Ph), 9.50 (s, br, 2H, NH). ^{13}C NMR ($CDCl_3$, δ, ppm): 12.32, 12.89 (CH_3), 44.90 (N−CH_3), 46.25, 46.75 (N−CH_2), 127.70, 128.70, 131.47, and 132.86 (Ph), 148.96 (C=N), 179.73(C=S), 183.26 (C=S).

Data for H_2L1b ($R^1 = R^2 = Et$, $R^3R^4 = -(CH_2)_4-$). Yield: 60% (1.089 g). Anal. Calcd for $C_{17}H_{25}N_5S_2$: C, 56.17; H, 6.93; N, 19.26; S, 17.64%. Found: C, 55.98; H, 6.77; N, 18.80; S, 17.46%. IR (ν in cm^{-1}): 3140 m (N−H), 1625 s (C=N). ^{1}H NMR ($CDCl_3$, δ, ppm): 1.06 (t, J = 6.6 Hz, 3 H, CH_3), 1.19 (t, J = 6.6 Hz, 3 H, CH_3), 1.91 (s, 2 H, pyrrolidine CH_2), 2.01 (s, 2 H, pyrrolidine CH_2), 3.47 (s, 2 H, pyrrolidine NCH_2), 3.53 (q, J = 6.6 Hz, 2 H, NCH_2CH_3), 3.76 (s, 2 H, pyrrolidine NCH_2), 3.87 (q, J = 6.6 Hz, 2 H, NCH_2CH_3), 7.37−7.47 (m, 3 H, Ph), 7.86 (d, J = 8.0 Hz, 2 H, o-Ph), 9.75 (s, br, 2H, NH). ESI MS (m/z): 386 $[M + Na]^+$, 402 $[M + K]^+$.

Data for H_2L1c ($R^1 = R^2 = Et$, $R^3R^4 = -(CH_2)_5-$). Yield: 52% (0.989 g). Anal. Calcd for $C_{18}H_{27}N_5S_2$: C, 57.26; H, 7.21; N, 18.55; S, 16.98%. Found: C, 56.90; H, 7.24; N, 18.48; S, 16.99%. IR (ν in cm^{-1}): 3194 m (N−H), 1628 s (C=N). ^{1}H NMR ($CDCl_3$, δ, ppm): 1.07 (t, J = 6.5 Hz, 3 H, CH_3), 1.21 (t, J = 6.6 Hz, 3 H, CH_3), 1.65 (m, 6 H, piperidine CH_2), 3.56 (q, J = 6.5 Hz, 2 H, NCH_2CH_3), 3.80 (s, 4 H, piperidine NCH_2), 3.86 (q, J = 6.5 Hz, 2 H, NCH_2CH_3), 7.38−7.48 (m, 3 H, Ph), 7.84 (d, J = 8.5 Hz, 2 H, o-Ph), 10.10 (s, br, 2H, NH). ESI MS (m/z): 378 $[M + H]^+$, 400 $[M + Na]^+$, 416 $[M + K]^+$.

Data for H_2L1d ($R^1 = R^2 = Et$, $R^3R^4 = -(CH_2)_6-$). Yield: 60% (1.173 g). Anal. Calcd for $C_{19}H_{29}N_5S_2$: C, 58.27; H, 7.46; N, 17.88; S, 16.38%. Found: C, 59.12; H, 7.40; N, 17.19; S, 16.82%. IR (ν in cm^{-1}): 3186 m (N−H), 1632 s (C=N). ^{1}H NMR ($CDCl_3$, δ, ppm): 1.05 (t, J = 7.1 Hz, 3 H, CH_3), 1.27 (t, J = 7.1 Hz, 3 H, CH_3),1.52 (s, br, 4 H, CH_2), 1.79 (s, br, 4 H, CH_2), 3.56 q, J = 7.0 Hz, 2 H, N−CH_2), 3.64 N(s, 2 H, azepine −CH_2), (q, J = 7.0 Hz, 2 H, N−CH_2), 3.93 (q, J = 7.1 Hz, 2 H, N−CH_2), 4.00 (s, 2 H, azepine −CH_2), 7.41−7.51 (m, 3 H, Ph), 7.89 (d, J = 7.0 Hz, 2 H, o-Ph), 9.81 (s, br, 2H, NH). ^{13}C NMR ($CDCl_3$, δ, ppm): 12.25, 12.87 (CH_3), 26.73 (CH_2), 28.04 (CH_2), 45.56, 46.25 (N−CH_2), 58.20 (N−CH_2), 127.64, 128.64, 131.39 and 132.81(Ph), 148.93 (C=N), 178.76(C=S), 183.10 (C=S).

Data for H_2L1e ($R^1 = R^2 = Et$, $R^3 = Me$, $R^4 = Ph$). Yield: 39% (0.781 g). Anal. Calcd for $C_{20}H_{25}N_5S_2$: C, 60.12; H, 6.31; N, 17.53; S, 16.05%. Found: C, 58.95; H, 6.13; N, 18.42; S, 15.95%. IR (ν in cm^{-1}): 3317 m, 3171 (N−H), 1628 s (C=N). ^{1}H NMR ($CDCl_3$, δ, ppm): 1.13 (t, J = 7.1 Hz, 3 H, CH_3), 1.22 (t, J = 7.2 Hz, 3 H, CH_3), 3.40 (m, 4 H, NCH_2CH_3), 3.58 (s, 3 H, NCH_3), 7.1−7.4 (m, 8 H, Ph), 7.82 (d, J = 8.0 Hz, 2 H, Ph). ESI MS (m/z): 400 $[M + H]^+$, 422 $[M + Na]^+$, 438 $[M + K]^+$.

Data for H_2L2d (R^1R^2 = -($CH_2CH_2OCH_2CH_2$)-, R^3R^4 = -$(CH_2)_6$-). Yield: 74% (1.498 g). Anal. Calcd for $C_{19}H_{27}N_5OS_2$: C, 56.27; H, 6.71; N, 17.27; S, 15.81%. Found: C, 56.17; H, 6.59; N, 17.24; S, 15.90%. IR (ν in cm^{-1}): 3201 (N−H), 1630 s (C=N). ^{1}H NMR ($CDCl_3$, δ, ppm): 1.51 (s, br, 4 H, CH_2), 1.77 (s, br, 4 H, CH_2), 3.4−4.1(m, 12H, N−CH_2), 7.32−7.47 (m, 3 H, Ph), 7.85 (d, J = 7.8 Hz, 2 H, o-Ph), 9.60 (s, br, 2H, NH).

Syntheses of [ReOCl(L1)] (1) and [ReOCl(L2)] (2). H_2L (0.1 mmol) dissolved in 3 mL MeOH was dropwise added to a stirred solution of $(NBu_4)[ReOCl_4]$ (58 mg, 0.1 mmol) in 2 mL MeOH. The color of the solution immediately turned deep red, and a red precipitate deposited within a few minutes. The red powder was filtered off, washed with cold methanol, and recrystallized from CH_2Cl_2/MeOH.

Data for 1a ($R^1 = R^2 = Et$, $R^3 = R^4 = Me$). Yield: 84% (48 mg). Elemental analysis: Calcd for $C_{15}H_{21}ClN_5OReS_2$: C, 31.43; H, 3.69; N, 12.22; S, 11.19%. Found: C, 31.35; H, 3.64; N, 12.19; S, 11.05%. IR (ν in cm^{-1}): 1519 vs (C=N), 984 s (Re=O). ^{1}H NMR ($CDCl_3$, δ, ppm): 1.36, 1.39 (t, J = 7.2 Hz, 3 H, CH_3), 3.16 (s, 6 H, N−CH_3), 3.99 (m, 4 H, CH_2), 7.38 (t, J = 7.7 Hz, 2 H, Ph), 7.43 (t, J = 7.2 Hz, 1 H, Ph), 7.68 (d, J = 7.5 Hz, 2 H, o-Ph). ^{13}C NMR ($CDCl_3$, δ, ppm): 13.12, 13,21 (CH_3), 41.88 (N−CH_3), 47.12, 47.52 (N−CH_2), 127.66, 130.63, 131.30, 136.43 (Ph), 166.94 (C=N), 168.90 (C=S), 169.73 (C=S).

Data for 1b ($R^1 = R^2 = Et$, $R^3R^4 = -(CH_2)_4-$). Yield: 80% (48 mg). Elemental analysis: Calcd for $C_{17}H_{23}ClN_5OReS_2$: C, 34.08; H, 3.87; N, 11.69; S, 10.70%. Found: C, 33.95; H, 3.59; N, 11.39; S, 11.01%. IR (ν in cm^{-1}): 1520 vs (C=N), 980 s (Re=O). ^{1}H NMR ($CDCl_3$, δ, ppm): 1.20 (m, 6 H, CH_3), 1.86 (s, 4 H, CH_2), 3.41 (s, 4 H, pyrrolidine NCH_2), 3.5−3.9 (m, 4 H, NCH_2), 7.30−7.37 (m, 3 H, Ph), 7.67 (d, J = 7.0 Hz, 2 H, o-Ph). ESI MS (m/z): 596 (5%) $[M - Cl^- + MeOH]^+$, 618 (100%) $[M - HCl + MeOH + Na]^+$.

Data for 1c ($R^1 = R^2 = Et$, $R^3R^4 = -(CH_2)_5-$). Yield: 76% (46 mg). Elemental analysis: Calcd for $C_{18}H_{25}ClN_5OReS_2$: C, 35.26; H, 4.11; N, 11.42; S, 10.46%. Found: C, 35.33; H, 3.98; N, 11.26; S, 11.01%. IR (ν in cm^{-1}): 1519 vs (C=N), 979 s (Re=O). ^{1}H NMR ($CDCl_3$, δ, ppm): 1.34 (t, J = 6.0 Hz, 3 H, CH_3), 1.39 (t, J = 6.0 Hz, 3 H, CH_3), 1.58 (m, 6 H, CH_2), 3.66 (s, 4 H, piperidine NCH_2), 3.8−4.1 (m, 4 H, NCH_2), 7.35 (t, J = 7.3 Hz, 2 H, Ph), 7.42 (t, J = 7.3 Hz, 1 H, Ph), 7.63 (d, J = 7.7 Hz, 2 H, o-Ph). ESI MS (m/z): 610 (20%) $[M - Cl^- + MeOH]^+$, 632 (100%) $[M - HCl + MeOH + Na]^+$, 648 (15%) $[M - HCl + MeOH + K]^+$.

Data for 1d ($R^1 = R^2 = Et$, $R^3R^4 = -(CH_2)_6-$). Yield: 71% (45 mg). Elemental analysis: Calcd for $C_{19}H_{27}ClN_5OReS_2$: C, 36.38; H, 4.34; N, 11.17; S, 10.22%. Found: C, 36.43; H, 4.34; N, 11.15; S, 10.14%. IR (ν in cm^{-1}): 1527 vs (C=N), 983 s (Re=O). ^{1}H NMR ($CDCl_3$, δ, ppm): 1.37 (t, J = 7.2 Hz, 3 H, CH_3), 1.42 (t, J = 7.1 Hz, 3 H, CH_3), 1.54 (m, 4 H, CH_2), 1.67 (s, 4 H, CH_2), 3.69 (m, 4 H, azepine N−CH_2), 4.00 (m, 4 H, N−CH_2), 7.34−7.44 (m, 3 H, Ph), 7.65 (d, J = 8.0 Hz, 2 H, o-Ph). ^{13}C NMR ($CDCl_3$, δ, ppm): 13.16, 13.21 (CH_3), 26.87 (CH_2), 28.34 (CH_2), 47.10, 47.47 (N−CH_2), 52.77 (N−CH_2), 127.63, 130.51, 131.10, 136.38 (Ph), 166.66 (C=N), 168.81 (C=S), 168.79 (C=S). ESI MS (m/z): 624 (25%) $[M - Cl^- + MeOH]^+$, 646 (100%) $[M - HCl + MeOH + Na]^+$, 662 (15%) $[M - HCl + MeOH + K]^+$.

Data for 1e ($R^1 = R^2 = Et$, $R^3 = Me$, $R^4 = Ph$). Yield: 62% (39 mg). Elemental analysis: Calcd for $C_{20}H_{23}ClN_5OReS_2$: C, 37.82; H, 3.65; N, 11.03; S, 10.09%. Found: C, 37.88; H, 3.81; N, 11.26; S, 10.30%. IR (ν in cm^{-1}): 1530 vs (C=N), 984 s (Re=O).

Table 5. X-ray Structure Data Collection and Refinement Parameters

	H_2L1b	[ReO(L1b)Cl] (**1b**)	[ReO(L1d)Cl] (**1d**)	[ReO(L1e)Cl] (**1e**)	[ReN(L1d)(PPh_3)] (**3d**)
formula	$C_{17}H_{25}N_5S_2$	$C_{17}H_{23}ClN_5OReS_2$	$C_{19}H_{27}ClN_5OReS_2$	$C_{20}H_{23}ClN_5OReS_2$	$C_{37}H_{42}N_6PReS_2$
M_w	363.54	599.02	627.23	635.20	852.06
crystal system	monoclinic	monoclinic	monoclinic	monoclinic	monoclinic
a/ Å	15.27(1)	10.982(1)	9.234(1)	9.671(1)	14.763(1)
b/ Å	13.408(4)	21.900(1)	10.908(1)	10.765(1)	25.552(1)
c/ Å	18.94(1)	9.524(1)	11.795(1)	22.184(1)	20.082(1)
α/ deg	90	90	90	90	90
β/ deg	99.55(7)	113.76(1)	106.74(1)	92.35(1)	107.04(1)
γ/ deg	90	90	90	90	90
V/ Å^3	3824(4)	2096.5(3)	1137.7(2)	2307.5(3)	7243.1(7)
space group	$P2_1/c$	$P2_1/c$	$P2_1$[a]	$P2_1/c$	$C2/c$
Z	4	4	2	4	8
$D_{calc.}$/g cm^{-3}	1.263	1.898	1.831	1.828	1.563
μ/mm^{-1}	0.287	6.140	5.662	5.585	3.550
no. of reflections	28246	15000	8488	14080	40089
no. of independent	10304	5624	6038	6192	9792
no. parameters	433	246	263	272	425
R1/wR2	0.0648/0.1189	0.0520/0.1165	0.0459/0.1122	0.0621/0.1605	0.0456/0.1004
GOF	0.920	0.970	1.028	0.958	1.008
deposit number	CCDC-728378	CCDC-728379	CCDC-728380	CCDC-728381	CCDC-728382

[a] Flack parameter: 0.043(14)

^{1}H NMR ($CDCl_3$, δ, ppm): 1.35 (m, 6 H, CH_3), 3.40 (s, 3 H, N−CH_3), 3.9−4.0 (m, 4 H, N−CH_2), 7.21 (m, 3 H, Ph), 7.28 (t, J = 7.5 Hz, 2 H, Ph), 7.40 (m, 3 H, Ph), 7.69 (d, J = 8.1 Hz, 2 H, Ph). ESI MS (*m*/*z*): 654 (90%) [M − HCl + MeOH + Na]$^+$, 670 (100%) [M − HCl + MeOH + K]$^+$.

Data for 2d (NR^{1}R^2 = Morph, R^{3}R^4 = -(CH$_2$)$_6$-). Yield: 78% (50 mg). Elemental analysis: Calcd for $C_{19}H_{25}ClN_5O_2ReS_2$: C, 35.59; H, 3.93; N, 10.92; S, 10.00%. Found: C, 35.45; H, 3.84; N, 10.77; S, 10.03%. IR (ν in cm^{-1}): 1524 vs (C═N), 981 s (Re═O). ^{1}H NMR ($CDCl_3$, δ, ppm): 1.55 (s, 4 H, CH_2), 1.69 (s, 4 H, CH_2), 3.4−4.2 (m, 12 H, N−CH_2), 7.31−7.42 (m, 3 H, Ph), 7.69 (d, J = 8.1 Hz, 2 H, o-Ph).

Syntheses of [ReN(L1)(PPh$_3$)] (3) and [ReN(L2)(PPh$_3$)] (4). A mixture of H_2L (0.1 mmol), [$ReNCl_2(PPh_3)_2$] (0.1 mmol), and three drops of Et_3N in CH_2Cl_2 (10 mL) was stirred at room temperature for 2 h, whereupon a clear red solution was obtained. The solvent was removed to dryness, the residue was washed with MeOH, and then dried under vacuum. The products were collected as red, analytically pure powders.

Data for 3a (R^1 = R^2 = Et, R^3 = R^4 = Me). Yield: 69% (55 mg). Elemental analysis: Calcd for $C_{33}H_{36}N_6PReS_2$: C, 49.67; H, 4.55; N, 10.53; S, 8.04%. Found: C, 49.63; H, 4.50; N, 10.39; S, 8.01%. IR (ν in cm^{-1}): 1508 vs (C═N), 1099 m (Re≡N). ^{1}H NMR ($CDCl_3$, δ, ppm): 1.05 (t, J = 7.0 Hz, 3 H, CH_3), 1.15 (t, J = 7.1 Hz, 3 H, CH_3), 2.95 (s, 6 H, N−CH_3), 3.68 (m, 4 H, NCH_2), 7.2−7.7 (m, 20 H, Ph). ^{31}P{H} NMR ($CDCl_3$, δ, ppm): 33.47. ESI MS (*m*/*z*): 799 (100%) [M + H]$^+$.

Data for 3d (R^1 = R^2 = Et, R^{3}R^4 = -(CH$_2$)$_6$-). Yield: 68% (58 mg). Elemental analysis: Calcd for $C_{37}H_{42}N_6PReS_2$: C, 52.15; H, 4.97; N, 9.86; S, 7.53%. Found: C, 51.99; H, 4.84; N, 9.70; S, 7.62%. IR (ν in cm^{-1}): 1508 vs (C═N), 1099 m (Re≡N). ^{1}H NMR ($CDCl_3$, δ, ppm): 1.06 (t, J = 7.0 Hz, 3 H, CH_3), 1.17 (t, J = 7.0 Hz, 3 H, CH_3), 1.41 (s, 4 H, CH_2), 1.47 (s, 4 H, CH_2), 3.51 (t, 4H, azepine N−CH_2) 3.66 (m, 4 H, NCH_2), 7.2−7.8 (m, 20 H, Ph). ^{31}P{H} NMR ($CDCl_3$, δ, ppm): 33.69. ESI MS (*m*/*z*): 853 (100%) [M + H]$^+$, 875 (100%) [M + Na]$^+$.

Data for 4d (NR^{1}R^2 = Morph, R^{3}R^4 = -(CH$_2$)$_6$-). Yield: 64% (56 mg). Elemental analysis: Calcd for $C_{37}H_{40}N_6OPReS_2$: C, 51.31; H, 4.66; N, 9.70; S, 7.40%. Found: C, 51.23; H, 4.71; N, 9.64; S, 7.34%. IR (ν in cm^{-1}): 1498 vs (C═N), 1095 m (Re≡N). ^{1}H NMR ($CDCl_3$, δ, ppm): 1.46 (s, 4 H, CH_2), 1.60 (s, 4 H, CH_2), 3.4−3.9 (m, 12 H, N−CH_2), 7.2−7.9 (m, 20 H, Ph). ^{31}P{H} NMR ($CDCl_3$, δ, ppm): 33.12.

X-ray Crystallography. The intensities for the X-ray determinations were collected on a STOE IPDS 2T instrument with Mo Kα radiation (λ = 0.71073 Å) at 200 K. Standard procedures were applied for data reduction and absorption correction. Structure solution and refinement were performed with SHELXS97 and SHELXL97.[14] Hydrogen atom positions were calculated for idealized positions and treated with the "riding model" option of SHELXL. More details on data collections and structure calculations are contained in Table 5. Additional information on the structure determinations has been deposited with the Cambridge Crystallographic Data Centre.

Biochemicals and Biological Studies

Cell Culture Conditions. The human MCF-7 breast cancer cell line was obtained from the American type Culture Collection (ATCC). This cell line was maintained as a monolayer culture in L-glutamine containing Dulbeccòs Modified Eaglès Medium (DMEM) with 4.5 g/L glucose (PAA Laboratories GmbH, Austria), supplement with 10% fetal calf serum (FCS; Gibco, Germany) using 25 cm^2 culture flasks in a humidified atmosphere (5% CO_2) at 37 °C. The cell lines were passaged twice a week after previous treatment with trypsin (0.05%)/ethylenediaminetetraacetic acid (0.02% EDTA; Boehringer, Germany). Jurkat cells were purchased from German Collection of Microorganisms and Cell Culture (Deutsche Sammlung von Mikroorganismen and Zellkulturen, Braunschweig), DSMZ No ACC 282, LOT 7. The cells were maintained in RPMI 1640 (PAA) medium supplemented with 10% fetal calf serum (PAA), 37 °C, 5% CO_2 and maximum humidity.

***In Vitro* Chemosensitivity Assay.** The *in vitro* testing of the substances for antitumor activity in adherent growing cell lines was carried out on exponentially dividing human cancer cells according to a previously published microtiter assay.[15] Exponential cell growth was ensured during

(14) Sheldrick, G. M. *SHELXS-97 and SHELXL-97, programs for the solution and refinement of crystal structures*; University of Göttingen, Göttingen, Germany, 1997.

(15) (a) Bernhart, G.; Reile, H.; Birnböck, H.; Spruss, T.; Schönenberger, H. *Cancer Res. Clin. Oncol.* **1992**, *118*, 35. (b) Reile, H.; Birnböck, H.; Bernhardt, G.; Spruss, T.; Schönenberger, H. *Anal. Biochem.* **1990**, *187*, 262.

the whole time of incubation. Briefly, 100 μL of a cell suspension was placed in each well of a 96-well microtiter plate at 7200 cells/mL of culture medium and incubated at 37 °C in a humidified atmosphere (5% CO_2) for 3 d. By removing the old medium and adding 200 μL of fresh medium containing an adequate volume of a stock solution of metal complex, the desired test concentration was obtained. Cisplatin was dissolved in dimethylformamide (DMF) while dimethylsulfoxide (DMSO) was used for all other compounds. Eight wells were used for each test concentration and for the control, which contained the corresponding amount of DMF and DMSO, respectively. The medium was removed after reaching the appropriate incubation time. Subsequently, the cells were fixed with a solution of 1% (v/v) glutaric dialdehyde in phosphate buffered saline (PBS) and stored under PBS at 4 °C. Cell biomass was determined by means of a crystal violet staining technique as described earlier.[16] The effectiveness of the complexes is expressed as corrected T/C_{corr} [%] or τ[%] values according to the following equation:

$$\text{cytostatic effect} : T/C_{corr}[\%] = [(T - C_0)/(C - C_0)] \times 10$$

$$\text{cytocidal effect} : \tau[\%] = [(T - C_0)/C_0] \times 100$$

whereby T (test) and C (control) are the optical densities at 590 nm of crystal violet extract of the cells in the wells, that is, the chromatin-bound crystal violet extracted with ethanol (70%) with C_0 being the density of the cell extract immediately before treatment. For the automatic estimation of the optical density of the crystal violet extract in the wells, a microplate autoreader (Flashscan S 12; Analytik Jena, Germany) was used.

Acknowledgment. H.H.N. gratefully acknowledges PhD grants from the government of Vietnam. Financial support of DFG − Deutsche Forschungsgemeinschaft (project: FOR 630), DAAD, CAPES, and FAPESP are appreciated.

Supporting Information Available: Crystallographic data in CIF file format. This material is available free of charge via the Internet at http://pubs.acs.org.

(16) Marmur, J. A. *J. Mol. Biol.* **1961**, *3*, 208.